

Metallicity measurements of GRB explosion sites: lessons from H II regions in M31

Yuu Niino^a, Kentaro Nagamine^{bc} and Bing Zhang^c

^a*Division of Optical & Infrared Astronomy, National Astronomical Observatory of Japan
2-21-1 Osawa, Mitaka, Tokyo 181-8588, Japan*

^b*Department of Earth and Space Science, Graduate School of Science, Osaka University
1-1 Machikaneyama-cho, Toyonaka, Osaka, 560-0043, Japan*

^c*Department of Physics and Astronomy, University of Nevada, Las Vegas
4505 S. Maryland Pkwy, Las Vegas, NV 89154-4002, U.S.A.*

E-mail: yuu.niino@nao.ac.jp

We examine how the small-scale variation of metallicity within a galaxy, which is found in nearby galaxies, affect the observational estimates of metallicity in the explosion sites of gamma-ray bursts (GRBs). Assuming the same luminosity, metallicity, and spatial distributions of H II regions as observed in M31, we compute the apparent metallicities that we would obtain when the spectrum of a target region is blended with those of surrounding H II regions within the length scale of typical spatial resolution. When the spatial resolution is \gtrsim a few kpc, we always obtain the apparent metallicity of $12+\log(\text{O}/\text{H}) \sim 8.8$ (average metallicity of H II regions in M31) regardless of the actual metallicities of the target regions (which has a wide range of $12+\log(\text{O}/\text{H}) = 8.1\text{--}9.3$ for the M31 H II regions). Our results suggest that current observational estimates of high-metallicity for some long-GRB environments do not rule out the hypothesis that long GRBs are exclusively born in low-metallicity environment.

*Swift: 10 Years of Discovery
2-5 December 2014
La Sapienza University, Rome, Italy*

1. Introduction

Some theoretical studies on the origin of long-duration gamma-ray bursts (long GRBs) using stellar evolution models suggest that a low metallicity may be a necessary condition for a GRB to occur ($Z < \text{a few} \times 0.1Z_{\odot}$ [1, 2]). Observational studies have also shown that the metallicity distribution of the GRB host galaxies at redshifts $z \lesssim 1$ is significantly biased towards lower metallicities than that of general late-type galaxies at similar redshifts [3, 4]. However, the metallicity of a host galaxy is not necessarily identical to that of the progenitor of a stellar explosion that occurs in it. There might be systematic differences between metallicities of the host galaxies and the progenitors [5]. To address this issue, some observational studies tried to spatially resolve some GRB host galaxies and measure the metallicity of the local environment at the GRB sites [6]. The systematic metallicity differences between the transient event sites and other parts of the host galaxies are actually observed in some cases [7]. On the other hand, it is also claimed that the explosion sites of some GRBs have high metallicities [8].

It is not known what spatial resolution is necessary to probe the immediate environment of a transient, which would be closely connected to the nature of the progenitor star. Especially for GRBs that typically occur at redshifts $\gtrsim \text{a few} \times 0.1$, the typical spatial resolution of ground-based observations (~ 1 arcsec) corresponds to a few kpc. Therefore it is likely that there is some metallicity variation below the resolution limit. Recent observations of local galaxies have begun to unveil the internal metallicity structure of galaxies at a few hundred pc scale. In particular, Sanders et al. (2012, hereafter S12) [9] obtained the spectra of > 200 H II regions (HIIRs) in M31 (the Andromeda galaxy), and found that $\sim 1/3$ of the HIIR pairs with separations less than 500 pc show significant (i.e., larger than the error) metallicity variation.

Here we briefly discuss how the metallicity estimates from spectroscopic observations are affected by limited resolution (see Niino, Nagamine & Zhang 2014 [10] for more detailed discussion). We do this by performing mock blended observations with limited resolution, assuming the same observed distributions of emission-line luminosities and line ratios as the M31 HIIRs.

2. Properties of the H II regions

We use the observed properties of the HIIRs in M31 to investigate how the spatial resolution limit affect the metallicity estimates of explosion site. Azimlu et al. (2011, hereafter A11) [11] constructed a photometric sample of HIIRs based on broad and narrow band images taken by the Local Group Galaxies Survey (LGGS [12]) covering the whole disk of M31. The sample contains 3961 HIIRs with $H\alpha$ luminosities $L_{H\alpha} \gtrsim 10^{34.5} \text{ erg s}^{-1}$, excluding known and potential planetary nebulae (PNe). The largest spectroscopic sample of HIIRs in M31 was constructed by S12, who obtained spectra of 253 HIIRs and 407 PNe, selected from the LGGS images and some samples of emission line objects in the literature.

We use the N2 index = $\log_{10}[\text{N II}]/H\alpha$ (hereafter [N II] means [N II] $\lambda 6584$ unless specified otherwise) as an indicator of metallicity with the empirical calibration by Nagao et al. (2006) [13] to maximize our sample size with metallicity estimates. Among the 253 HIIRs in the S12 sample, $H\alpha$ and [N II] lines are detected for 223 HIIRs, while $R_{23} = ([\text{O II}] \lambda 3727 + [\text{O III}] \lambda 4959 + [\text{O III}] \lambda 5007)/H\beta$, which is also a popular metallicity indicator, is available only for 61 HIIR. S12 confirmed that the

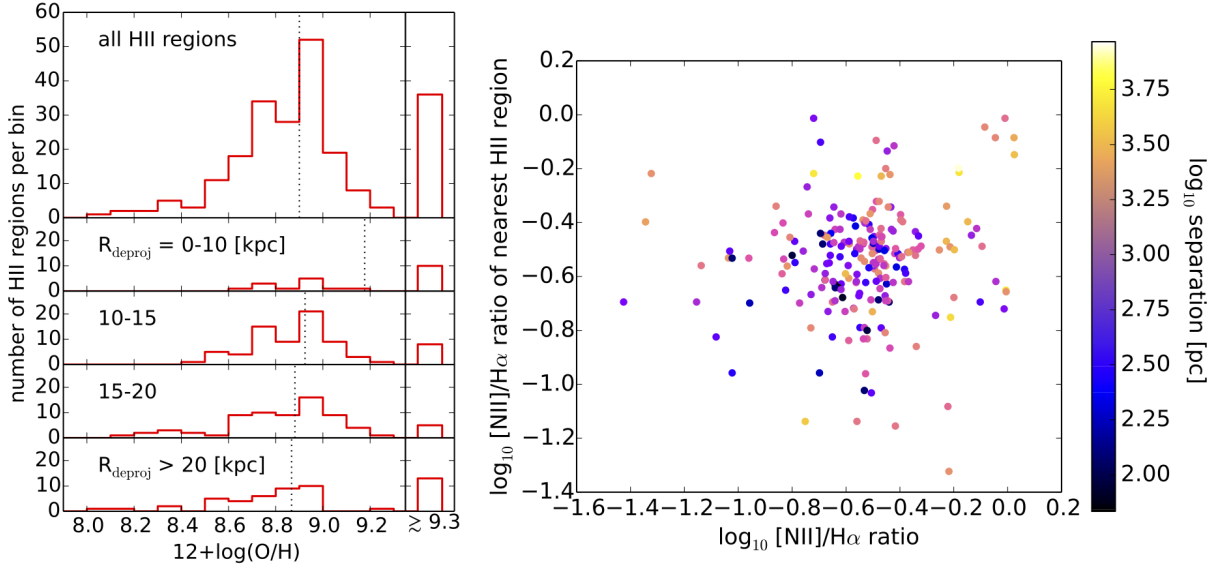


Figure 1: *Left:* metallicity distribution of the M31 HIIRs in the S12 sample, measured with the N2 index calibrated by Nagao et al. (2006) [13]. The top panel shows the distribution of all M31 HIIRs, and the other panels show the distributions at deprojected galactocentric radii $R_{\text{deproj}} = 0\text{--}10$, $10\text{--}15$, $15\text{--}20$ and > 20 kpc. The number of HIIRs with $N2 > -0.38$ (i.e. $12+\log(O/H) \gtrsim 9.3$) is shown separately in the right-hand-side of each panel. The vertical dotted lines represent the median of each distributions including the HIIRs with $N2 > -0.38$. *Right:* comparison of the N2 indices of each HIIR and the nearest one in the S12 sample. Separations of the HIIR pairs on the disk of M31 are colour-coded from dark blue (close, ~ 100 pc) to bright yellow (distant, ~ 8 kpc).

HIIR metallicity distribution measured with the N2 index agrees with that measured with most of other popular calibration methods.

We show the metallicity distribution of all M31 HIIRs in the top one of the left panels of Figure 1. In the bottom 4 of the left panels of Figure 1, the sample is divided into 4 subsamples according to the deprojected galactocentric radius (R_{deproj}). The HIIR metallicities at larger R_{deproj} are systematically lower. The large intrinsic scatter of metallicity discussed in S12 is clearly seen in each R_{deproj} bin.

S12 pointed out that 33% of the close HIIR pairs (with deprojected separations < 0.5 kpc) show metallicity variation of more than 0.3 dex. To further investigate the metallicity variation on small scales, we compare the N2 index of each HIIR and the nearest one for which N2 index is available (the right panel of Figure 1). We do not find any significant correlation between the N2 indices of the neighboring HIIR pairs including the cases with the deprojected separation of a few 100 pc. This suggests that the ISM in M31 is not mixed efficiently, and that the ISM metallicity varies even on small scales of a few 100 pc.

It should be noted that S12 obtained the line fluxes with 1.5 arcsec fibers, and the fiber loss corrected total luminosity is not available in the S12 sample. To obtain the emission line luminosities of the S12 HIIRs, we match the S12 sample to the photometric sample of A11. Although the spectroscopic observations are performed only for a small fraction of the detected HIIRs, the sample with $H\alpha$ and $[N\text{II}]$ detections covers a wide range of line luminosity, $35.0 <$

$$\log_{10} L_{\text{H}\alpha + [\text{N II}]} [\text{erg s}^{-1}] < 37.5.$$

3. Metallicity measurements with limited spatial resolutions

In this section, we discuss what spatial resolution would be necessary to obtain a reliable metallicity for a GRB site, and how the observed metallicities differ from the intrinsic ones under the observations with insufficient spatial resolution. In the following, we define the ‘‘apparent metallicity’’ of a HIIR for a resolution scale radius of R_{res} as a metallicity inferred from the ratio of total $\text{H}\alpha$ and $[\text{N II}]$ line fluxes of all HIIRs inside R_{res} .

As mentioned in §2, the sampling rate of spectroscopic sample is low, and the N2 index is not available for most A11 HIIRs. For demonstration purposes, we assume that the HIIRs with unknown N2 index follows the same N2 index distribution as found in the S12 sample. We divide the S12 sample into four different bins of R_{deproj} (0–10, 10–15, 15–20, and > 20 kpc, the left panels of Figure 1) and examine the effect of metallicity gradient.

Practically, the apparent metallicities are calculated as follows. For each HIIR with $\text{H}\alpha$ and $[\text{N II}]$ detections in S12, we collect all HIIRs from the A11 sample which reside within a given radius of R_{res} (deprojected), and sum up the $\text{H}\alpha$ and $[\text{N II}]$ fluxes. For an A11 HIIR that has a matched S12 HIIR with a known N2 index, the $\text{H}\alpha$ and $[\text{N II}]$ fluxes are calculated assuming the index value. When the N2 index is not available for an A11 HIIR, we randomly select an S12 HIIR in the same R_{deproj} bin with $\text{H}\alpha$ and $[\text{N II}]$ detections, and $\log_{10} L_{\text{H}\alpha} [\text{erg s}^{-1}] > 36.5$ (to avoid the effect of possible bias in the metallicity distribution of faint HIIRs [10]). Then we calculate the $\text{H}\alpha$ and $[\text{N II}]$ fluxes of the A11 HIIR assuming the same N2 index to that of the selected S12 HIIR. We repeat this random realization of apparent metallicities 100 times and obtain 100 apparent metallicities for each of HIIRs with $\text{H}\alpha$ and $[\text{N II}]$ detections.

We show the intrinsic versus apparent metallicities of HIIRs in Figure 2 for $R_{\text{res}} = 0.1, 0.3, 0.5, 1.0, 2.0,$ and 3.0 kpc. When $R_{\text{res}} \geq 1$ kpc, the HIIRs with lower (higher) intrinsic metallicities than $12 + \log(\text{O}/\text{H})_{\text{int}} = 8.8$ have systematically higher (lower) apparent metallicities than the intrinsic values. This is because most of the contaminating HIIRs have N2 indices that correspond to $12 + \log(\text{O}/\text{H}) = 8.7 - 9.0$ (the left panels of Figure 1). In this case, it is difficult to distinguish low-metallicity HIIRs from high-metallicity ones, because all HIIRs with intrinsic $12 + \log(\text{O}/\text{H})_{\text{int}} = 8.2 - 9.2$ have similar apparent metallicities within the scatter. When $R_{\text{res}} < 1$ kpc, the apparent metallicity correlates well with the intrinsic value, although some systematic differences exist for $R_{\text{res}} = 0.3$ and 0.5 kpc.

4. Conclusions

We examined how the small-scale metallicity variation in a galaxy affects the observations of GRB sites with limited spatial resolution, using the observational data of M31 HIIRs as a template of metallicity variation in a late-type galaxy. Our results suggest that, when the GRB sites are resolved down to $R_{\text{res}} \lesssim 500$ pc scale, the estimated apparent metallicities (or emission-line ratios) do reflect the immediate environment of the GRBs.

The detections of transient events with low event rate density (e.g., long GRBs) are rare in the local Universe, and we need to rely on a sample at higher redshifts, where $R_{\text{res}} \gtrsim$ a few kpc

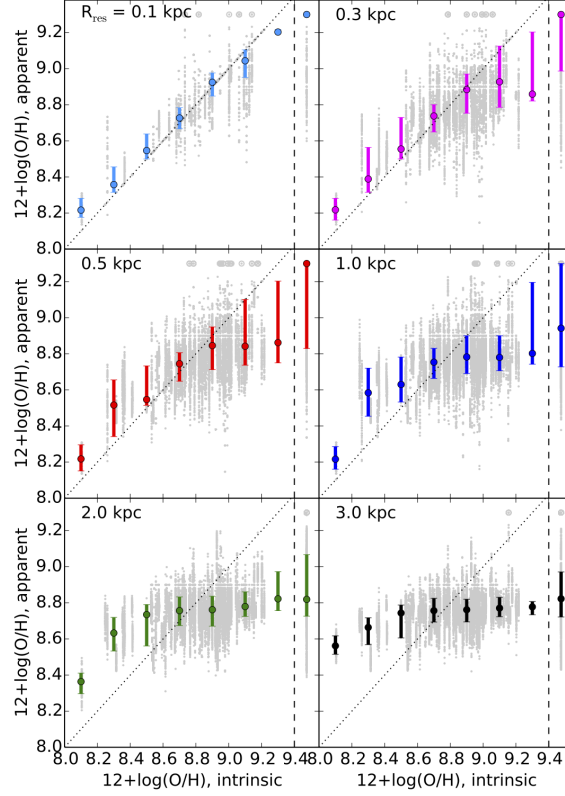


Figure 2: Intrinsic versus apparent metallicities of HIIRs with known N2 index for various R_{res} . The grey dots represent each data points. The grey circles at the top of each panel represent the data with apparent N2 > -0.38 . The data points with intrinsic N2 > -0.38 are plotted separately in the right-hand-side of each panel. The circles and the error bars indicate median and 68 percentile scatter of the data points in intrinsic metallicity bins (bin width of 0.2 dex). The data points with apparent N2 > -0.38 are included in the median and scatter calculation. The diagonal dotted line indicates the equality between the apparent and intrinsic metallicities.

typically. With such low spatial resolution, our results suggest that it is difficult to constrain the site metallicities accurately, and the measured HIIR metallicities will be close to the average metallicity of the host galaxy due to the blending within the spatial resolution.

Some of the host galaxies of long GRBs and the explosion sites are found to have high metallicities with limited spatial resolution of \gtrsim a few kpc [8, 14, 15]. However, low-metallicity star formation could still take place in a host galaxy with a high averaged metallicity. This means that the above observations do not rule out the hypothesis that long GRBs are exclusively born in a low-metallicity environment, as suggested by the stellar evolution models [1, 2].

Our results are based only on the observed statistical properties of the HIIRs in M31, however, HIIRs in other galaxies may have different properties to the M31 HIIRs. Many GRB host galaxies are in fact dwarf irregulars that actively form stars [16], and it is likely that they have different ISM properties from that of the spiral galaxies like M31. At the same time, some host galaxies

of long GRBs are spiral galaxies, which often have higher masses and metallicities than dwarf irregulars. These spiral galaxies are especially interesting in the context of metallicity dependence of long-GRB occurrence, and they may have similar HIIR properties to M31. Larger spectroscopic samples of HIIRs with very high spatial resolution of a few 10 pc in dwarf irregulars and other types of galaxies are necessary to further discuss the relation between the apparent and intrinsic metallicities in more general population of host galaxies.

References

- [1] Yoon, S., & Langer, N. 2005, *Evolution of rapidly rotating metal-poor massive stars towards gamma-ray bursts*, *A&A* **443** 643
- [2] Woosley, S. E., & Heger, A. 2006, *The progenitor stars of gamma-ray bursts*, *ApJ* **637** 914
- [3] Stanek, K. Z., et al. 2006, *Protecting life in the milky way: metals keep the GRBs away*, *Acta Astronomica* **56** 333
- [4] Graham, J. F., & Fruchter, A. S. 2013, *The metal aversion of LGRBs*, *ApJ* **774** 119
- [5] Niino, Y. 2011, *Revisiting the metallicity of long-duration gamma-ray burst host galaxies: the role of chemical inhomogeneity within galaxies*, *MNRAS* **417** 567
- [6] Modjaz, M., Kewley, L., Kirshner, R. P., Stanek, K. Z., Challis, P., Garnavich, P. M., Greene, J. E., Kelly, P. L., & Prieto, J. L., 2008, *Measured metallicities at the sites of nearby broad-lined type Ic supernovae and implications for the supernovae gamma-ray burst connection*, *AJ* **135** 1136
- [7] Levesque, E. M., Berger, E., Soderberg, A. M., & Chornock, R. 2011, *Metallicity in the GRB 100316D/SN 2010bh host complex*, *ApJ* **739** 23
- [8] Levesque, E. M., Kewley, L. J., Graham, J. F., & Fruchter, A. S. 2010, *A high-metallicity host environment for the long-duration GRB 020819*, *ApJL* **712**, L26
- [9] Sanders N. E., Caldwell N., McDowell J., & Harding P., 2012, *The metallicity profile of M31 from spectroscopy of hundreds of H II regions and PNe*, *ApJ* **758** 133 (S12)
- [10] Niino, Y., Nagamine, K., & Zhang, B. 2015, *Metallicity measurements of gamma-ray burst and supernova explosion sites: lessons from H II regions in M31*, *MNRAS* **449** 2706
- [11] Azimlu, M., Marciniak, R., & Barmby, P. 2011, *A new catalog of H II regions in M31*, *AJ* **142** 139 (A11)
- [12] Massey, P., Olsen, K. A. G., Hodge, P. W., Strong, S. B., Jacoby, G. H., Schlingman, W., & Smith, R. C. 2006, *A survey of local group galaxies currently forming stars. I. UBVR photometry of stars in M31 and M33*, *AJ* **131** 2478
- [13] Nagao, T., Maiolino, R., & Marconi, A. 2006, *Gas metallicity diagnostics in star-forming galaxies*, *A&A* **459** 85
- [14] Niino, Y., Hashimoto, T., Aoki, K., Hattori, T., Yabe, K., & Nomoto, K. 2012, *GRB 100418A: a long GRB without a bright supernova in a high-metallicity host galaxy*, *PASJ* **64** 115
- [15] Elliott, J., et al. 2013, *The low-extinction afterglow in the solar-metallicity host galaxy of γ -ray burst 110918A*, *A&A* **556** A23
- [16] Le Floc'h, E., et al. 2003, *Are the hosts of gamma-ray bursts sub-luminous and blue galaxies?*, *A&A* **400** 499